Nuclear Instruments and Methods in Physics Research A276 (1989) 258–262
North-Holland, Amsterdam

A PARALLEL PLATE CHAMBER WITH PIXEL READOUT PARTICULARLY SUITABLE FOR VERY HIGH DATA RATE

F. ANGELINI, R. BELLAZZINI, A. BREZ, M.M. MASSAI and M.R. TORQUATI

Dipartimento di Fisica dell' Università di Pisa and Istituto Nazionale di Fisica Nucleare, Sezione di Pisa, Via Livornese 582/A, San Piero a Grado, 56010 Pisa, Italy

Received 2 May 1988 and in revised form 5 September 1988

We report the preliminary test results on the performance of a device especially designed for the imaging of X rays at a very high data rate. A prototype having 256 readout channels has been built and tested in our lab. The detector is a two-step parallel plate chamber. The anode is made up of a chess board of pads, onto which a thin germanium layer is evaporated to restore the electrical continuity. Each individual pad can be read out independently on the back of the board.

1. Introduction

To be suitable for X-ray imaging a gas detector should satisfy the following stringent requirements: (i) a good detection efficiency, (ii) a good spatial resolution, (iii) a high data rate capability. To satisfy the first requirement one has to use a gas with a high atomic number (i.e. xenon) possibly at high pressure. For the second requirement the use of a monochromatic X-ray source with energy just above the xenon K or L edge can greatly help, together with high pressure to achieve a submillimeter spatial resolution. The rate capability is therefore the true bottleneck. The rate performance in a gas detector is limited by two factors: space-charge effects and the speed of the electronic readout chain. The classical MWPC used in X-ray measurement generally suffers from these space charge effects. The rate limit for an MWPC is about 10^4 counts/s mm [1]. At least two orders of magnitude increase is needed to cope with the counting rate requirements of, for example, synchrotron radiation imaging. It seems that the problem can be solved by a device with a parallel plate chamber (PPC) structure [2,3]. The important difference from an MWPC structure is that the PPC electrostatic field is not concentrated around single thin wires but is constant over the entire amplification volume. The first consequence is that the space-charge effect is drastically reduced. This is due to the combined effect of (i) the spatial spread of the amplification process over the entire detector volume and (ii) the very short drift time of the positive ions across the amplification gap. The second advantage of such a structure is the x–y symmetry. Therefore, the problem still to be solved is the speed of the electronic readout system which has to cope with a rate requirement as high as 10^5 counts/pixel s.

We can classify a readout system as: (i) global, that is, looking at the detector as a whole, or (ii) subdivided, that is, highly parallel with each individual resolution element (or pixel) working asynchronously with the others. A global readout system can be made highly interpolating between the individual readout elements, thus allowing for a high spatial resolution. However, because the readout system must manage the whole rate, a severe limitation on the data acquisition speed immediately arises (typical speed can range between 0.1 and 1 MHz). A subdivided, parallel system seems more appropriate when the speed of the data taking is the major requirement. For this reason we have tested in our laboratory a prototype of a PPC in which individual anode pads (256 out of a total of 16000) are read out independently. For this preliminary laboratory investigation discrete elements are utilized but use of VLSI technology is planned for the readout of the whole chamber. Each channel will work at 100 kHz speed so that a 1.6 GHz global speed should be achieved.

2. The device

The PPC (see fig. 1) is made of two parts: an ionization and drift region, 5 mm thick, followed by a much thinner amplification region (2 mm thick) having a parallel plate structure. A 20 μm thick nickel mesh having 600 line pairs/in. (manufactured by Buckbee–Mears Operation, Minneapolis, USA) divides the two field regions. The transparency of the nickel mesh is 100% at the operating ratio of the electric field intensity in the drift and amplification region [4]. The anode of the parallel plate chamber is made of a chess board of 16000 pads having a 0.9 mm side and 0.1 mm

apart, onto which a thin germanium layer is evaporated to restore the dc electrical continuity. The fine pitch of the cathode grid and the deposition of a resistive layer onto the anode pads were chosen to have the maximum uniformity of the electrical field avoiding any residual modulation as much as possible [5]. The surface resistance depends on the thickness of the germanium coating. In our case it was $\approx 100\ k\Omega/\square$. The resistive layer prevents also the space-charge buildup in the nonconducting region between the pads. A metallized hole of 0.2 mm diameter electrically connects each individual anode pad to its replica on the back of the board. A thin insulated copper wire of 0.15 mm diameter is glued onto the readout pad on the back of the board making use of a conductive glue (see fig. 2). This wire connects each pad to a current preamplifier mounted directly on the chamber box. The glueing procedure consists of the following steps: (1) the PPC anode is put under an optical microscope ($\times 10$), (2) the 1 mm long enamel cover of the end of the copper wire is removed by means of chemical stripping, (3) the one millimeter end of the wire is immersed in a conductive glue (Chomerics, Wobur, MA, USA), so that a small drop of the viscous glue adheres to the wire, (4) the end of the wire is put in the 1 mm deep metallized hole and fixed. Steps 2–4 are repeated for all of a row (12 pads). The glue is then left to dry for half an hour at $\approx 100\,^{\circ}C$ temperature and the process is started again for the second row (21 total). The whole glueing process took 2 days at an experienced operator. For these tests, the standard gas filling was argon (80%) and CO_2 (20%). Carbon dioxide was selected for its low transversal diffusion. A typical operating voltage was 3.0 kV for the amplification gap while the drift gap was operated between 500–1500 V.

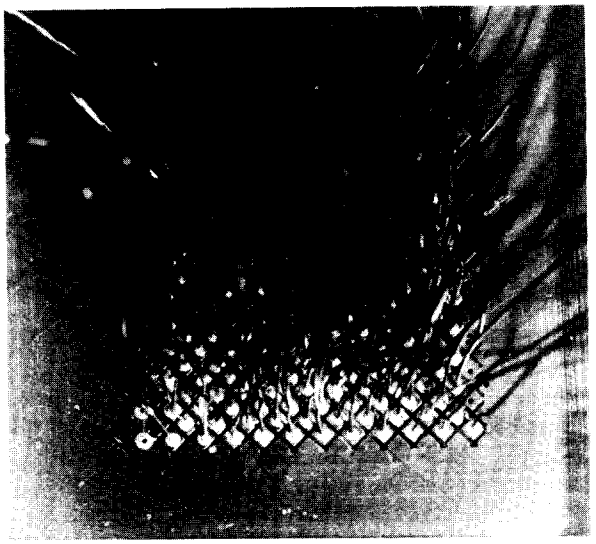

Fig. 2. A magnified detail of the anode pads and of the electrical connections.

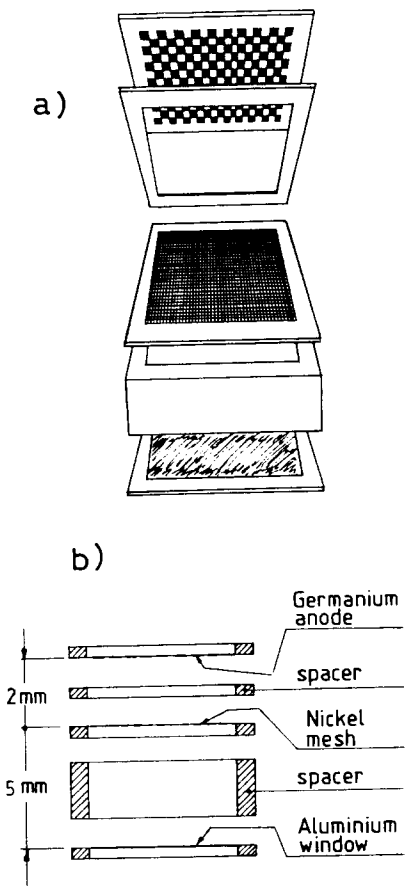

Fig. 1. (a) An exploited view of the detector assembly; (b) a cross section of the detector.

3. The readout system

To exploit the rate capability of the device, the final readout system will be made of completely asynchronous elements (pre- and post-amplifier, discriminator and memory scaler for each pad). We are now designing this electronic chain that will make use of custom VLSI technology. For the present test the readout electronic chain is based on an RMH (receiver memory hybrid module) system [6]. Eight preamplifier modules are mounted directly on the detector and each drive 32 twisted pair cables which serve also as delay element (400 ns) between the pad signal and the read out trigger. The RMHs amplify the received signals and, in case of a valid even, strobe them into the memory. The data acquisition is started by the prompt signal obtained from the mesh plane. For each valid event, the signal on the pads is readout and processed, via a Camac interface, by an IBM PC-AT computer.

4. Results of laboratory test

Fig. 3 shows an example of the pad signal obtained with a ^{55}Fe source uniform illumination. The rise and fall time are set by the RMH preamplifier which has an input impedance of 700 Ω. The FWHM of the 5.9 keV peak was 25% at an estimated gas gain $G \approx 5 \times 10^4$. The current signal is ≈ 1 μA and it lasts 5 μs [2]. For each pad event there will be a local, negligible, 100 mV voltage drop, lasting 5 μs. Because the mean time interval between pad events will be 10 μs, no rate problem should come from the resistive coating. This is a beneficial effect of the rate subdivision between independent channels. To study the spatial resolution, we have built a resolution phantom consisting of two slits 100 μm wide, 0.5 cm thick and 1.8 mm apart. It was illuminated uniformly by a ^{55}Fe source. Fig. 4a shows the reconstructed image of the two slits. The detector is operated in a digital mode, i.e. the output signal from each pad is compared with a threshold and if higher than that threshold the number of counts of the interested pad is increased by one. Fig. 4b is the histogram obtained when projecting the two-dimensional image of fig. 4a along the vertical axis. It represents the line spread function of this digital detector. The background which is seen in fig. 4b is probably due to the absorption of the 3 keV fluorescent line of argon far from the primary interaction point.

5. Experimental and Monte Carlo study of the multihit problem

An important parameter that has to be studied is the number of near pad hits in each event. Indeed, if the data acquisition speed is not the major requirement, advantage can be taken from having more than one pad hit. Local or global interpolation algorithms can be devised, unavoidably at the expense of the rate. If, as in our case, the data rate is the most important point, multihits can be a serious problem when quantitative imaging is required. In fig. 5 the measured number (%) of multihits versus the energy threshold is reported (^{55}Fe source illumination). We have investigated the dependence of chamber response (efficiency, multihits) as a function of several variables (geometrical and physical) by means of a Monte Carlo program. This program models the process of absorption the impinging radiation (5.9 keV X-ray) with the filling gas (Ar, Xe, CO_2), the subsequent random clustering ionization, the drift movement of electrons toward the anode and the distribution of the collected charge an anode pads. It is therefore possible to optimize the design of the detector in terms of gap thickness, pressure, gas filling, etc. In particular, we have studied the multihit fraction, i.e. the number of events in which there is more than one pad which has collected a charge greater than a

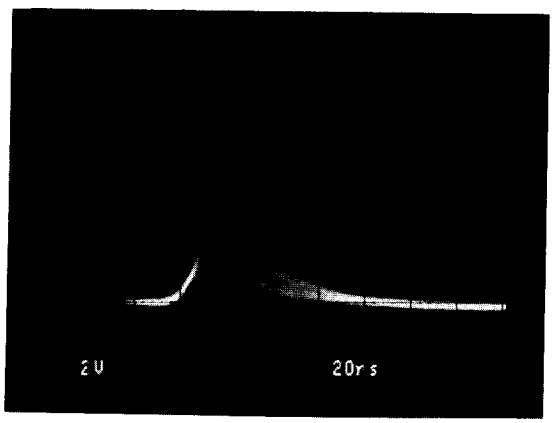

Fig. 3. A typical pad signal obtained when the chamber is irradiated with a ^{55}Fe source. The signal rise and fall time are set by the RMH amplifier.

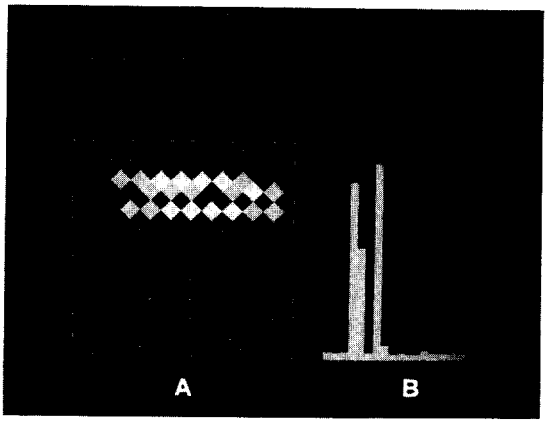

Fig. 4. (a) The reconstructed image of two slits 100 μm wide, 1.8 mm apart, (b) the histogram obtained when projecting the image of (a) along the vertical axis.

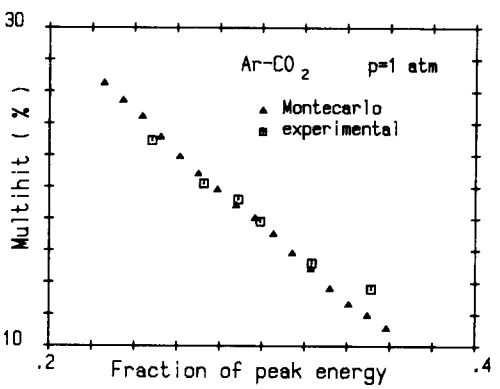

Fig. 5. The number (%) of multihits versus energy threshold (Monte Carlo and experimental).

Table 1
Monte Carlo parameters (1 atm)

Gas mixture	$Ar-CO_2$	$Xe-CO_2$
$\langle n(e^-)\rangle$/event	230	270
λ (5.9 keV) (cm)	2.1	0.26
Photoel. range (μm)	100	70
$\sigma_\perp$ (1 e^{-1}) (μm) 1 cm drift space	200	200
Density (g/cm^3)	1.66×10^{-3}	5.49×10^{-3}
CO_2 (%)	20	20
Sensitive area (cm^2)	12.8×12.8	12.8×12.8

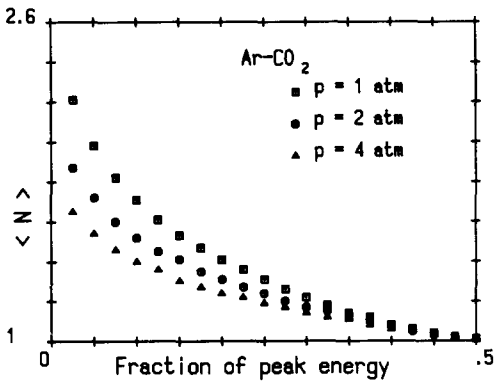

Fig. 6. The mean number of pads with signal over the threshold, i.e. with a charge larger than a preset fraction of the total ionization charge versus the threshold itself, for a drift region 1 cm thick and for different values of pressure in an $Ar-CO_2$ mixture.

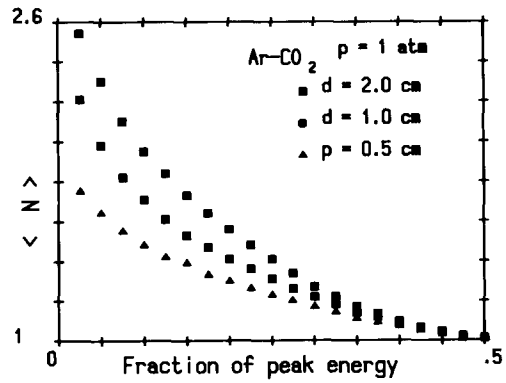

Fig. 7. The same as in fig. 6 but at fixed pressure (1 atm) and different drift region thicknesses.

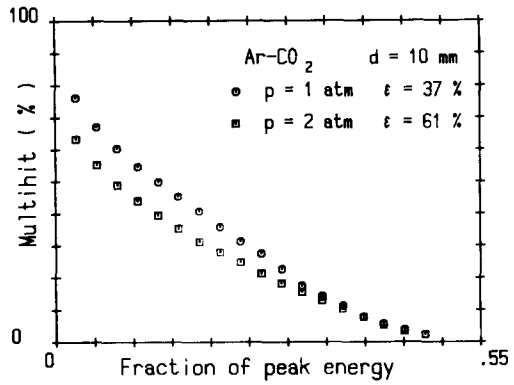

Fig. 8. The multihit fraction in an argon–CO_2 mixture at 1 and 2 atm.

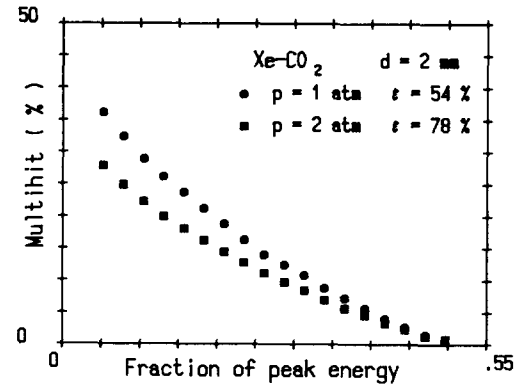

Fig. 9. The multihit fraction in a xenon–CO_2 mixture at 1 and 2 atm.

preset fraction of the total ionization charge, as function of the fraction itself. Table 1 reports the values of several parameters which were used in the Monte Carlo program. Simulating a uniform irradiation of the detector and following all processes up to the charge collection, we have obtained the charge distribution on the pads. Figs. 6 and 7 show the mean number of pads with signal over the threshold as function of the threshold itself. Fig. 8 shows the multihit fraction in an $Ar-CO_2$ mixture. Fig. 9 shows the large improvement which can be obtained using a xenon mixture. Because of the very short photon mean free path the drift space can be reduced to a few millimeters still having a detection efficiency higher than 50%. With a threshold of about 30%, a drift space of 2 mm and a pressure of 2 atm, the multihit fraction is reduced to a few per cent. The consequent reduction of efficiency due to the threshold is about 2%.

6. Conclusions

We have presented the preliminary results of a device specially designed for very high data rate applica-

tions. The rate capability has been increased, subdividing the readout system as much as possible (1 pixel/mm^2). This has been made possible by the continuous structure of a PPC. The extrapolation to a full-scale device needs the integration of VLSI electronics on the detector itself.

References

[1] F. Sauli, CERN Report no. 77/09 (1977).
[2] J. Hendrix et al., Nucl. Instr. and Meth. 252 (1986) 246.
[3] R. Bellazzini et al., Nucl. Instr. and Meth. 247 (1986) 445.
[4] O. Bunemann, Can. J. Research 27A (1949) 191.
[5] F. Angelini et al., IEEE Trans. Nucl. Sci. NS-34 (1987) 495.
[6] J.B. Lindsay et al., Nucl. Instr. and Meth. 156 (1978) 329.